

1 **Pedobarographic Statistical Parametric Mapping of plantar pressure data in new and**
2 **confident walking infants: a preliminary analysis**

3 Eleonora Montagnani^{A*}, Stewart C Morrison^A, Matyas Varga^A, Carina Price^B

4

5 ^A School of Health Sciences, University of Brighton, Darley Road, Eastbourne, United Kingdom

6 ^B Centre for Health Sciences Research, University of Salford, Frederick Road, Salford, United

7 Kingdom

8

9 ***Corresponding author:**

10 Eleonora Montagnani

11 Email: e.montagnani@brighton.ac.uk

12 Address: 204 Aldro Building, 49 Darley Road, Eastbourne, BN20 7UR, UK

13

14 **Word count: 3500**

15

16

17

18

19

20

21

22

23

24

25
26
27
28
29
30
31
32
33
34
35
36
37
38
39
40
41
42
43
44
45
46
47
48
49
50
51
52
53

Abstract

In infancy, plantar pressure data during walking has been investigated through regional approaches, whilst the use of pedobarographic Statistical Parametric Mapping (pSPM) has not been reported. Analysis of pressure data using pSPM is higher in resolution and could enhance understanding of foot function development providing novel insights into plantar pressure changes. This work aims to detail the implementation of the pSPM data processing framework on infants' pressure data, comparing plantar pressure patterns between new and confident walking steps. Twelve infants walked across an EMED-xi platform. Steps were extracted and imported into MATLAB for analysis. Maximum pressure pictures were transformed to point clouds and registered within and between participants with iterative closest point and coherent point drift algorithms, respectively. Root mean square error (RMSE) was calculated within both registrations as a quality measure. Pressure patterns were compared between new and confident walking using nonparametric-paired sample SPM1D t-test. RMSEs were under 1 mm for both registration algorithms. In the transition to confident walking, significantly increasing pressure was detected in the left central forefoot. Implementing pSPM to infants' pressure data was non-trivial, as several phases of data processing were required to ensure a robust approach. Our analysis highlighted the presence of significant changes in pressure in central left forefoot after 2.2 months of walking, which have never been reported in the literature before. This can be explained as previous regional analyses approaches in infancy considered the forefoot as whole, preventing detection of changes in its anatomical correspondences.

Keywords: pSPM, foot, plantar pressure, infants, gait

54 **1. Introduction**

55 Quantifying plantar pressure data as infants learn and master walking skills enhances knowledge of
56 the typical biomechanics of the foot throughout development, providing information related to foot
57 function changes.

58 The conventional approach to analysis and reporting infants' pressure data is regional analysis, which
59 has been adopted using three, five, six or seven regions of interest (ROIs) (Montagnani et al, 2021).
60 Traditional regional analysis software have been developed to be accessible without the need to
61 understand programming languages (e.g., MATLAB, Python), making it easy to implement for pressure
62 data processing. This ease in processing data comes with certain disadvantages, notably assumptions
63 relating to the statistical treatment of regional data as discrete, treating the regions of the foot
64 independently (Pataky and Goulermas, 2008). Furthermore, the use of regional analysis in infancy
65 presents limitations due to the ongoing foot development, which causes lack of clear anatomical
66 definition on the plantar surface and a lack of hypotheses relating to the ROIs typically analyzed in the
67 plantar pressure field.

68 Pedobarographic Statistical Parametric Mapping (pSPM) conducts statistical inference at the pixel
69 level in the spatial domain (Pataky and Goulermas, 2008), and it has been adopted already in adults
70 (McClymont et al., 2016; Oliveira et al., 2010; Pataky et al., 2008) and children (Phethean et al., 2014).
71 However, the use of pSPM in infants' pressure analysis has not been reported. Adopting pSPM could
72 be non-trivial in infancy, as foot placement on the pressure platform could be influenced by gait
73 variability, the testing protocol adopted, and the developmental characteristics of the infant's feet.
74 These factors lead to capturing steps highly irregular in shape and spatial orientation (Price et al.,
75 2017) that could make data processing challenging. Therefore, this study aimed to detail the
76 implementation of the pSPM processing framework on infants' pressure data. By undertaking this
77 work, we also aimed to compare pressure patterns of new and confident walking infants, providing a

78 preliminary set of novel information about plantar pressure patterns that could direct future research
79 in the field.

80

81 **2. Methods**

82 This study emerges from a longitudinal study which is part of the Great Foundation Initiative (Price et
83 al., 2018). Ethical approval was obtained from the ethics committees of the Schools of Health Sciences
84 at the University of Brighton (LHPSCREC 17-11) and the University of Salford (HSCR161779).

85 *2.1 Participants*

86 Twelve infants (5 female) were recruited via social media and local communities in the South East
87 (Brighton) and North West (Salford) of England. For data collection, infants came to the Human
88 Movement Laboratory of the respective Universities at the attainment of two stages of foot loading
89 (Price et al., 2018):

- 90 • New walking: infants able to take 3 to 5 steps independently: mean age (SD): 13.2 months
91 (1.0); weight: 10.8 (1.1) kg; foot length: 11.4 (0.8) cm; foot width: 5.4 (0.4).
- 92 • Confident walking: infants able to take 10-15 steps independently and confidently, interacting
93 with others, carrying toys while walking, navigating around objects: mean age (SD): 15.1
94 months (1.3); weight: 11.3 (1.2) kg; foot length: 12.0 (0.8) cm; foot width: 5.4 (0.5).

95 Infants were born full-term, without neurological and/or musculoskeletal conditions, impairment in
96 attaining walking stages or gross motor development deficiency. Once infants reached each stage,
97 parents were asked to book the visit within 21 days. At each visit, written informed consent was given
98 by parents.

99 *2.2 Testing procedure*

100 Plantar pressure data were collected using the EMED xl platform (4 sensors per cm², 100Hz; Novel,
101 Munich, Germany), embedded in a nursery-style environment (Price et al., 2018). After familiarizing
102 with the space, infants walked freely, in self-selected directions and speed, across the space, while HD
103 video was collected (Vicon Bonita 720c; Oxford, U.K./Logitech HD Pro Webcam).

104

105

106 *2.3 Data pre-processing pSPM framework*

107 Steps were extracted from the pressure trials in the EMED software and processed if the feet were
108 within the platform borders and did not miss extensive anatomical parts. Visual inspection of the
109 steps' stance phase was also performed to ensure processing of steps from full gait cycles. This was
110 necessary due to the diverse nature of foot contact of new and confident walking steps. Left feet (LF)
111 and right feet (RF) were processed and analyzed separately, assuming population-level asymmetry.
112 Three steps for each foot, for each participant at each stage were used for this work (n=144). Steps
113 were exported as ASCII text files (Novel Emascii software), and imported into MATLAB 2019a (The
114 Mathworks Inc, Natick, USA) as numeric matrices for data processing and analysis. Each MPP was then
115 positioned in a grid of 36x25 pixels, to standardize matrix dimensions of each MPP. Non-zero entries
116 of the MPPs corresponded to pixels containing pressure values.

117 *2.3.1 Transformation to point clouds*

118 MPPs were converted into point clouds (PC) using a built-in MATLAB function that transformed each
119 pixel into a point. Two-dimensional (2D) pressure matrices were flattened, obtaining 1-dimensional
120 (1D) pressure vectors.

121 *2.3.2 Within-subjects registration*

122 PCs were registered within subject (WS) to a chosen template, defined as the point cloud with the
123 highest number of points. PCs that were subject to registration will be referred to as sources. To

124 perform WS registration, a rigid iterative closest point (ICP) algorithm for PC registration was used
125 (Besl and McKay, 1992), in the form of a built in MATLAB function. However, the visual inspection of
126 the data highlighted highly variable shape and spatial orientation of the steps (Fig. 1). The ICP
127 algorithm is highly susceptible to local minima and its performance relies on the quality of the initial
128 pose of the PCs (Yang et al., 2015). For this reason, previous works has tried to improve its
129 implementation by performing initial coarse alignment of the data (Makadia et al., 2006; Rusu et al.,
130 2009). Therefore, an additional data processing passage was required prior to WS registration, to yield
131 optimal points overlap. This was obtain by vertically aligning the original MPPs using principal
132 component analysis (PCA), similarly to Kim et al. (2013).

133 [Figure 1 in here].

134 2.3.3 Computing axes of MPPs using principal component analysis (PCA)

135 Binary MPPs were created and matrices of each MPP were put in two vectors (a and b) as coordinates.
136 The means of a and b were calculated and subtracted from each index of the respective coordinates,
137 creating new vectors: A and B . This enabled to find the centroid of the MPP. Coordinates were
138 positioned in matrix, which covariance was calculated as:

$$139 \quad C = \begin{pmatrix} cov(A, A) & cov(A, B) \\ cov(B, A) & cov(B, B) \end{pmatrix}$$

140 (1)

141 Eigenvectors and eigenvalues of the covariance matrix were found and plotted as the principal axes
142 of the MPPs (Fig.2). To perform a counterclockwise rotation of the MPPs, θ was calculated as the angle
143 forming between the longest eigenvector (x_1) and the vector parallel (black dashed line) to the y -axis
144 passing through the centroid (y_1) (Fig.2), according to:

$$145 \quad \theta = atan(x_1, y_1)$$

146 (2)

147 Where *atan* is a built-in MATLAB function returning the inverse tangent (\tan^{-1}) of the ratio of x_1 and y_1
148 in radians. Once θ was calculated (2), it was applied in the rotational transformation matrix (3), having
149 the general form:

$$\begin{pmatrix} \cos\theta & -\sin\theta \\ \sin\theta & \cos\theta \end{pmatrix} \quad (3)$$

152 to enable counterclockwise rotation of the MPPs to vertical. Coordinates were then multiplied by the
153 resulting transformation matrix, obtaining vertically aligned MPPs (Fig.2).

154 [Figure 2 in here].

155 Once PCA was performed, the rotated MPPs were re-transformed to PCs, and WS registration was
156 achieved through the rigid ICP algorithm. Quality of WS registration pre and post PCA is also reported
157 (Appendix A, Fig.S1)

158 After WS registration, for each vertex of the template a built-in MATLAB function was used (based on
159 Euclidean distances) that returns the nearest neighbors of a query point in the input PC, to find
160 corresponding points between the sources and the WS template.

161 2.3.4 Averaging

162 Once aligned and registered WS, corresponding coordinates of PCs were averaged, resulting in one
163 mean PC per participant per foot (Phethean et al., 2014). This was performed to reduce the impact of
164 differences in shape and dimensions of the PCs (Fig. 1), and to enhance further steps of data
165 processing.

166 2.3.5 Between-subjects template computation and registration

167 To perform between subjects (BS) registration, an unbiased BS template was chosen as the foot with
168 length and width closest to the mean length and width of all the feet analyzed (Pataky et al., 2011).
169 The non-rigid coherent point drift (CPD) algorithm for PC registration was performed through a built-

170 in MATLAB function, to allow the shape of the PCs to change using a displacement field as
171 transformation. Next, the nearest neighbors of each vertex in the source PC were found in the
172 unbiased BS template to establish points' correspondences.

173 *2.4 Statistical analysis*

174 To determine registration quality, the root-mean-square error (RMSE) was calculated between the
175 source and the template (Pataky, 2012) for each step. RMSE values were transformed to mm and
176 mean and standard deviation (SD) were reported. Graphic representations of the registration quality
177 were also reported for both WS and BS registrations.

178 Analysis with SPM1D was conducted between sets of PCs of new and confident walking steps. This
179 was possible as pressure data was spatially aligned and nonparametric inference used (Pataky and
180 Goulermas, 2008). Analysis was conducted using a two-tailed, nonparametric paired sample SPM1D
181 t-test (<http://www.spm1d.org/>), with significance set as $\alpha=0.05$. A t-value was calculated at each point
182 of the PCs, defining an SPM t curve. As nonparametric inference was used, multiple comparison
183 corrections was performed using nonparametric permutation test, where the critical threshold was
184 based on the maximum test statistic value across the entire domain (Pataky, 2012). If the SPM t-curve
185 crossed this critical threshold (t critical) at any point, significant points were located (Pataky, 2012),
186 reflecting that pressure in those points is significantly different between new and confident walking
187 steps. However, SPM1D only supports critical test statistic calculation, thus cluster-specific p values
188 were not available. Nonparametric linear regression was also performed between body weight
189 (confounding variable) and plantar pressure at pixel level using SPM1D (Appendix A, Fig.S2).

190 **3. Results**

191 *3.1 Within and between subject registration quality*

192 With respect to registration accuracy, the mean (SD) RMSEs in the LF were 0.36 mm (0.09) and 0.39
193 mm (0.08) for WS and BS registration, respectively. In the RF, the mean (SD) RMSEs were 0.38 mm

194 (0.06) and 0.37 mm (0.05) for WS and BS registration, respectively. Visual representation of the
195 registration performances was also presented in Fig. 3.

196 Fig. 3 (A) demonstrated minimal non-overlapping points found on the lateral border of the heel and
197 the medial border of the hallux. Considering the BS registration, non-overlapping points were present
198 around the apex of the toes, around the foot periphery and between the heel and the midfoot (Fig. 3,
199 B).

200 [Figure 3 in here].

201 *3.2 Plantar pressure inference*

202 In the transition from new to confident walking, pSPM detected an area of significantly increasing
203 pressure in the central forefoot of the LF (Fig. 4). Significant differences in pressures were not
204 identified in the RF; however, the qualitative trends suggested the presence of increased pressure in
205 the central heel, medial to lateral forefoot and decreased in the hallux in both LF and RF (Fig. 4 and 5).

206 [Figure 4 in here].

207 [Figure 5 in here].

208 Regression analysis of the pixel-level data revealed the absence of statistically significant correlation
209 between the increasing body weight and plantar pressure in both feet (Appendix A, Fig.S2).

210 **4. Discussion**

211 This work reported details of the implementation of the pSPM approach to infants' pressure data, also
212 investigating changes in plantar pressure as walking experience increases.

213 *4.1 Methodological considerations*

214 The use of pSPM in infancy is important to provide clear and unbiased insights into foot development.
215 Traditional software for pressure data processing rely on the assumption that analysis is carried out
216 on data presenting geometrical and/or pressure gradient patterns of adults' feet (Ellis et al., 2011).

217 Although regional analysis is advantageous under certain circumstances (e.g., offloading), its use can
218 be debatable in the context of development, due to the ongoing anatomical and structural changes of
219 the infants' feet. These changes prevent the foot from acting typically as a functional unit and
220 therefore undermine the relevance of common ROI boundaries implemented in typically developed
221 feet. Therefore, by selecting a methodology that divides the foot into ROIs according to adults' feet
222 features, researchers imply that the infant foot is a well-developed functional unit, ignoring its
223 anatomical and functional characteristics.

224 Another important methodological aspect of this study is the testing protocol and its effect on
225 pressure data in infancy. Infants were able to walk freely and uninstructed as opposed to being
226 restricted to a straight line, causing inconsistent directions of foot progression and contact patterns.
227 Therefore, we anticipated the presence of a high intra, inter individual variability, and assumed the
228 presence of population-level asymmetry in gait and related pressure patterns, which is why both feet
229 were analyzed in this study.

230 The presence of intra and inter subject variability associated with the unrestrained testing protocol
231 could also contribute to reduced registration quality. However, the rigid ICP algorithm, enhanced by
232 PCA, yielded low RMSEs in both LF and RF. This can be due to the closer intra-individual
233 correspondences in feet dimensions. The quality of the WS registration was also shown in Fig. 3 (A),
234 where the optimal overlap of points suggests a satisfying performance of the ICP algorithm to the
235 present data set. Performance of CPD algorithm was slightly less accurate, considering the RMSE
236 values and the visual representation of the registration (Fig. 3, B). This could be explained by the high
237 inter-individual differences in foot dimensions and profile on the pressure platform. Nevertheless,
238 RMSEs were under 0.4 mm for both WS and BS registration, which, considering the mean foot length
239 and width, indicates good fit of the sources to the template. Moreover, the low SD reported in both
240 registrations suggested that the ICP and CPD algorithms performed consistently on the PCs, without
241 high between registration variations. These results suggest that the proposed methodology provided

242 an effective, high quality, and solid framework to implement pSPM to free walking pressure data in
243 infancy.

244 *4.2 Functional considerations*

245 This study suggests that after 2.2 months of independent walking experience, pressure significantly
246 increases in the central left forefoot during gait. This has also been previously identified between 4
247 and 7 years, and authors argued about anatomical foot changes taking place (Phethean et al., 2014).
248 In this work, anatomical foot development is unlikely to occur at a rate that would cause significant
249 differences in pressure to happen, due to the short period between stages of foot loading (2.2
250 months). Furthermore, our analysis revealed that the increasing body weight did not influence plantar
251 pressure data (Appendix A, Fig.S2). This could be due to the minimal increase in weight between new
252 and confident walking stages (+0.5 kg; ~ 5% of initial body weight), which occurred alongside a
253 corresponding ~5% increase in foot length. A previous comparison of infants (mean age: 23.5 (5.7)
254 months) identified statistically increasing pressure in the central forefoot between trials of walking
255 and running (Hennig and Rosenbaum, 1991). This could suggest that significant pressure changes in
256 the central left forefoot could be attributed to the increasing walking speed, as infants become more
257 experienced walkers. However, this was not quantified and reported as part of this research and would
258 require further exploration.

259 Significant increasing pressure in the central forefoot between these stages of foot loading has not
260 been reported in the literature before, and it could be due to different methodological approaches
261 adopted in this study compared to existing research. Bertsch et al. (2004) found that during the first
262 year of independent walking, the whole forefoot demonstrated significantly increasing pressure.
263 However, the exact anatomical location of such change was unknown due to the application of a whole
264 forefoot region. This implies that differences in pressure distribution could have been anywhere within
265 the boundaries of the forefoot, limiting considerations regarding plantar pressure changes in the
266 transition to confident walking. Increasing the resolution of the forefoot mask (e.g., lateral, central,

267 and medial forefoot) might lead to the detection of significant differences in the central forefoot.
268 However, statistical outcomes would be highly dependent on the ROI selected (definition and number
269 of ROIs), which causes arbitrary and inconsistent exploration of infants' pressure data, as reported
270 elsewhere (Montagnani et al, 2021).

271 Other changes in pressure were identified also qualitatively in both feet, and specifically in the central
272 heel, medial to lateral forefoot and hallux (Fig. 4 and 5, A, B). Previous works demonstrated that
273 pressure in the hallux is the highest during the first few months of independent walking but decreases
274 after three to six months of walking (Bertsch et al., 2004; Bosch et al., 2010; Hennig and Rosenbaum,
275 1991). The literature also report significant increasing heel pressure during the first year of
276 independent walking (Bertsch et al., 2004), as initial heel contact occurs as opposed to forefoot
277 contact (Hallemans et al., 2003; Hallemans et al., 2006). Findings from our work agree with previous
278 studies and suggest that changes in pressure occur rapidly, as infants become confident in walking. As
279 opposed to previous works reporting data in infancy for either LF, RF, or mixed (Alvarez et al., 2008;
280 Bertsch et al., 2004; Bosch et al., 2010), our work showed different statistical results in LF and RF. This
281 could be the related to the presence of high inter-limb asymmetry during the first months of walking
282 (Ledebt et al., 2004), which could lead to different pressure changes in the RF and LF between early
283 and confident walking. However, because a large area of non-significant pressure increase is visible in
284 the RF (Fig. 5), differences in statistical outcomes might in-fact be due to the small sample size
285 analyzed, in terms of both the number of participants and steps included in the analysis. This could
286 also explain why we were not able to detect larger areas of significant changes in pressure in either
287 foot during the transition to confident walking. Combining pressure data from LF and RF by mirroring
288 would have provided a larger sample size, but this would have assumed population-level symmetry in
289 gait and related pressure patterns within the loading stages.

290 Thus, additional work should be undertaken to investigate whether differences in pressure are present
291 between LF and RF within foot loading stages, which would illuminate population-level symmetry in

292 plantar pressure patterns. Future research analyzing a larger sample with pSPM may have the
293 capability to detect the presence of plantar pressure changes that have not been reported before.
294 Therefore, further investigations with the present methodology are warranted, to increase resolution
295 of data analysis and ensure clearer understanding of foot function development, as infants become
296 confident in walking.

297 **Acknowledgment**

298 At the time this article was written, Eleonora Montagnani and Matyas Varga were PhD students at the
299 Department of Health Sciences at the University of Brighton, England, funded by The Dr William M
300 Scholl Unit of Podiatric Development.

301 **References**

- 302 Alvarez, C., De Vera, M., Chhina, H., Black, A., 2008. Normative data for the dynamic pedobarographic
303 profiles of children. *Gait Posture* 28, 309-315.
- 304 Bertsch, C., Unger, H., Winkelmann, W., Rosenbaum, D., 2004. Evaluation of early walking patterns
305 from plantar pressure distribution measurements. First year results of 42 children. *Gait & Posture* 19,
306 235-242.
- 307 Besl, P.J., McKay, N.D., Year Method for registration of 3-D shapes. In *Sensor fusion IV: control*
308 *paradigms and data structures*.
- 309 Bosch, K., Gerss, J., Rosenbaum, D., 2010. Development of healthy children's feet--nine-year results of
310 a longitudinal investigation of plantar loading patterns. *Gait Posture* 32, 564-571.
- 311 Ellis, S.J., Stoecklein, H., Yu, J.C., Syrkin, G., Hillstrom, H., Deland, J.T., 2011. The accuracy of an
312 automasking algorithm in plantar pressure measurements. *HSS Journal*® 7, 57-63.
- 313 Hallemans, A., D'Août, K., De Clercq, D., Aerts, P., 2003. Pressure distribution patterns under the feet
314 of new walkers: the first two months of independent walking. *Foot & ankle international* 24, 444-453.

315 Hallemans, A., De Clercq, D., Van Dongen, S., Aerts, P., 2006. Changes in foot-function parameters
316 during the first 5 months after the onset of independent walking: a longitudinal follow-up study. *Gait*
317 *Posture* 23, 142-148.

318 Hennig, E.M., Rosenbaum, D., 1991. Pressure distribution patterns under the feet of children in
319 comparison with adults. *Foot & ankle* 11, 306-311.

320 Kim, C., Son, H., Kim, C., 2013. Fully automated registration of 3D data to a 3D CAD model for project
321 progress monitoring. *Automation in Construction* 35, 587-594.

322 Ledebt, A., van Wieringen, P.C., Savelsbergh, G.J., 2004. Functional significance of foot rotation
323 asymmetry in early walking. *Infant Behavior and Development* 27, 163-172.

324 Makadia, A., Patterson, A., Daniilidis, K., Year Fully automatic registration of 3D point clouds. In 2006
325 IEEE Computer Society Conference on Computer Vision and Pattern Recognition (CVPR'06).

326 McClymont, J., Pataky, T.C., Crompton, R.H., Savage, R., Bates, K.T., 2016. The nature of functional
327 variability in plantar pressure during a range of controlled walking speeds. *Royal Society open science*
328 3, 160369.

329 Oliveira, F.P., Pataky, T.C., Tavares, J.M.R., 2010. Registration of pedobarographic image data in the
330 frequency domain. *Computer methods in biomechanics and biomedical engineering* 13, 731-740.

331 Pataky, T.C., 2012. Spatial resolution in plantar pressure measurement revisited. *Journal of*
332 *biomechanics* 45, 2116-2124.

333 Pataky, T.C., Bosch, K., Mu, T., Keijsers, N.L., Segers, V., Rosenbaum, D., Goulermas, J.Y., 2011. An
334 anatomically unbiased foot template for inter-subject plantar pressure evaluation. *Gait Posture* 33,
335 418-422.

336 Pataky, T.C., Caravaggi, P., Savage, R., Parker, D., Goulermas, J.Y., Sellers, W.I., Crompton, R.H., 2008.
337 New insights into the plantar pressure correlates of walking speed using pedobarographic statistical
338 parametric mapping (pSPM). *Journal of biomechanics* 41, 1987-1994.

339 Pataky, T.C., Goulermas, J.Y., 2008. Pedobarographic statistical parametric mapping (pSPM): a pixel-
340 level approach to foot pressure image analysis. *Journal of biomechanics* 41, 2136-2143.

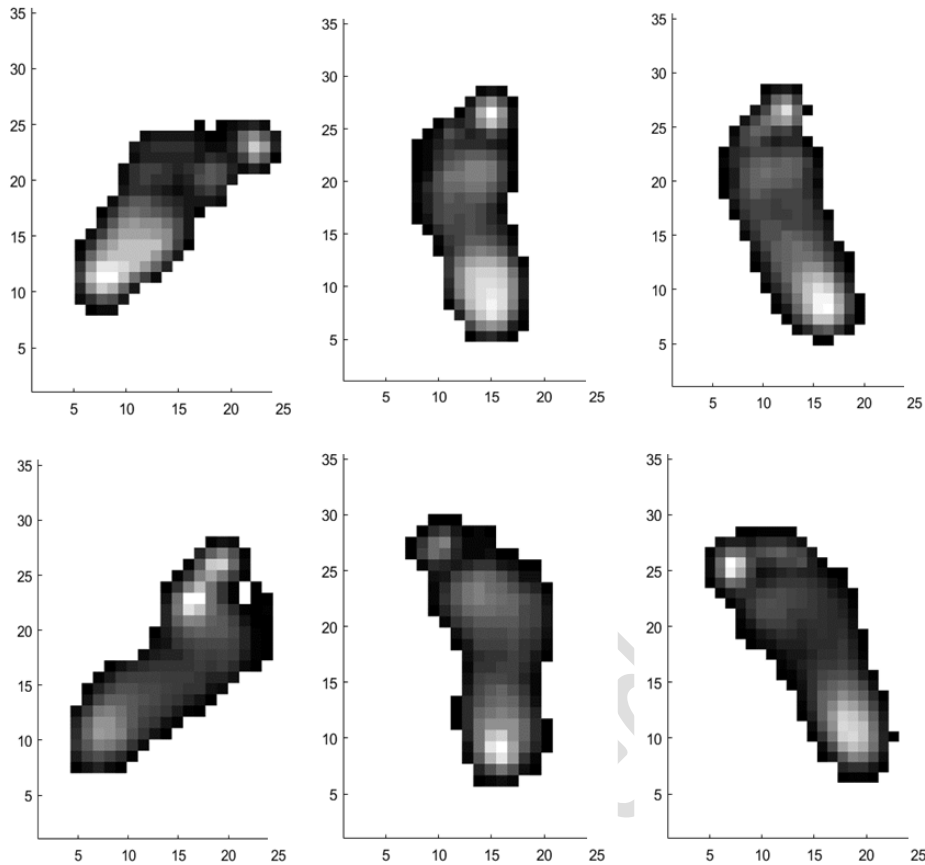
341 Phethean, J., Pataky, T.C., Nester, C.J., Findlow, A.H., 2014. A cross-sectional study of age-related
342 changes in plantar pressure distribution between 4 and 7 years: a comparison of regional and pixel-
343 level analyses. *Gait Posture* 39, 154-160.

344 Price, C., McClymont, J., Hashmi, F., Morrison, S.C., Nester, C., 2018. Development of the infant foot
345 as a load bearing structure: study protocol for a longitudinal evaluation (the Small Steps study). *J Foot
346 Ankle Res* 11, 33.

347 Price, C., Morrison, S.C., Nester, C., 2017. Variability in foot contact patterns in independent walking
348 in infants. *Footwear Science* 9, S47-S49.

349 Rusu, R.B., Blodow, N., Beetz, M., Year Fast point feature histograms (FPFH) for 3D registration. In
350 2009 IEEE international conference on robotics and automation.

351 Yang, J., Li, H., Campbell, D., Jia, Y., 2015. Go-ICP: A globally optimal solution to 3D ICP point-set
352 registration. *IEEE transactions on pattern analysis and machine intelligence* 38, 2241-2254.



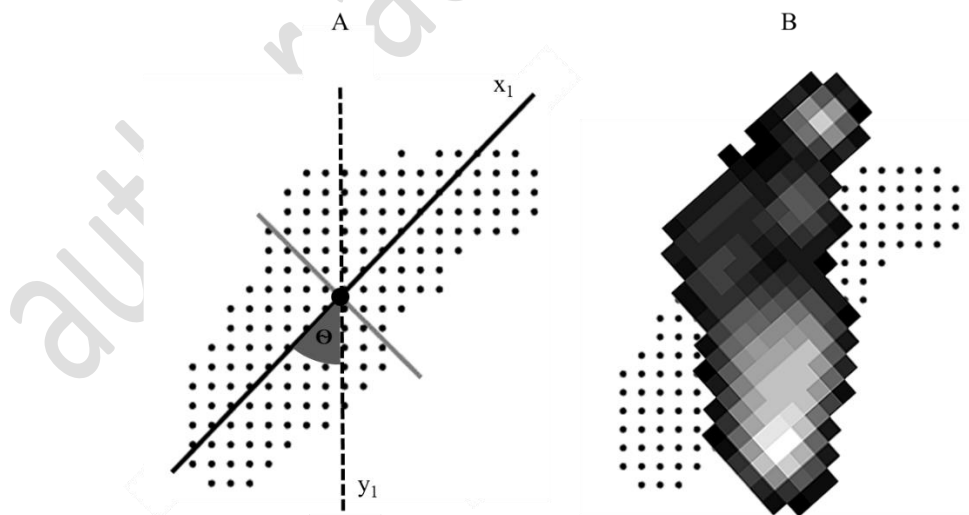
353

354

355

Fig. 1. Example of the spatial orientation of left and right MPPs positioned in a common reference system of 36x25 pixels.

356



357

358

359

360

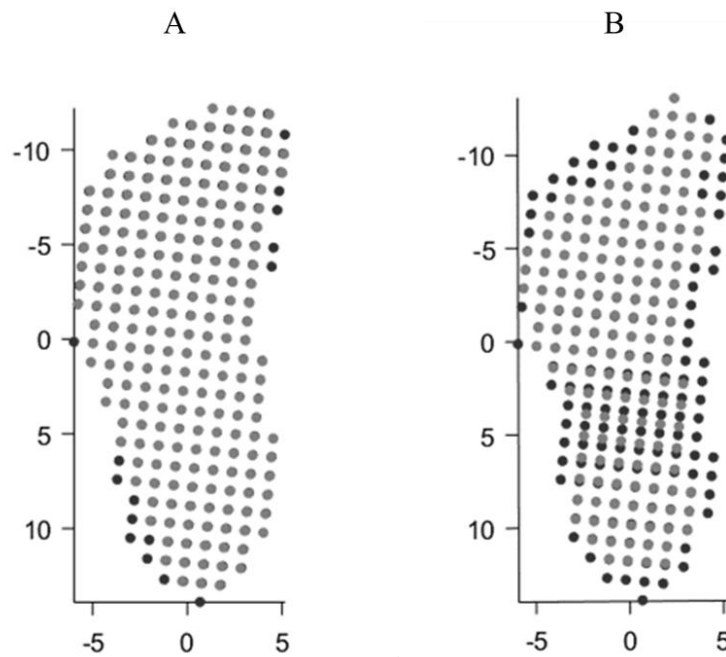
361

362

Fig. 2. (A) non-aligned MPP (black dots), principal axes are identified as black (x_1) and grey lines intersecting at the image centroid, where the vector parallel to the y -axis passes through (y_1); x_1 and y_1 were used to calculate Θ . The grey, shorter axis was reported for display purposes, enabling to visualize the centroid of the MPP, thus the intersecting point of y_1 . (B) Non-aligned binary MPP (black dots) and vertically aligned MPP (greyscale, pixel-image).

363

364



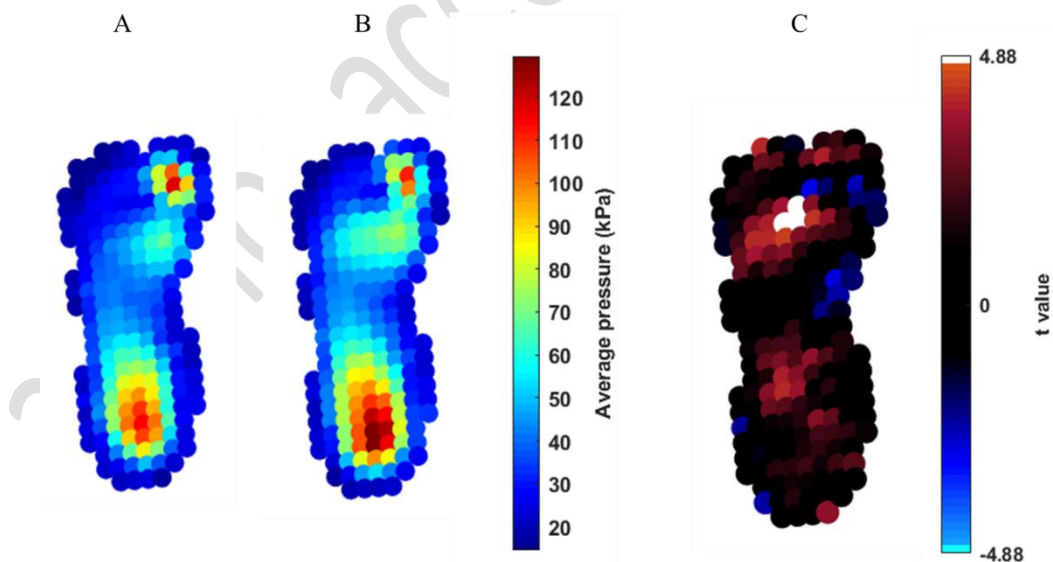
365

366

367

Fig. 3. Visual representation of the source (grey points) and template (black points) overlap during WS registration (A) and BS registration (B).

368



369

370

371

372

373

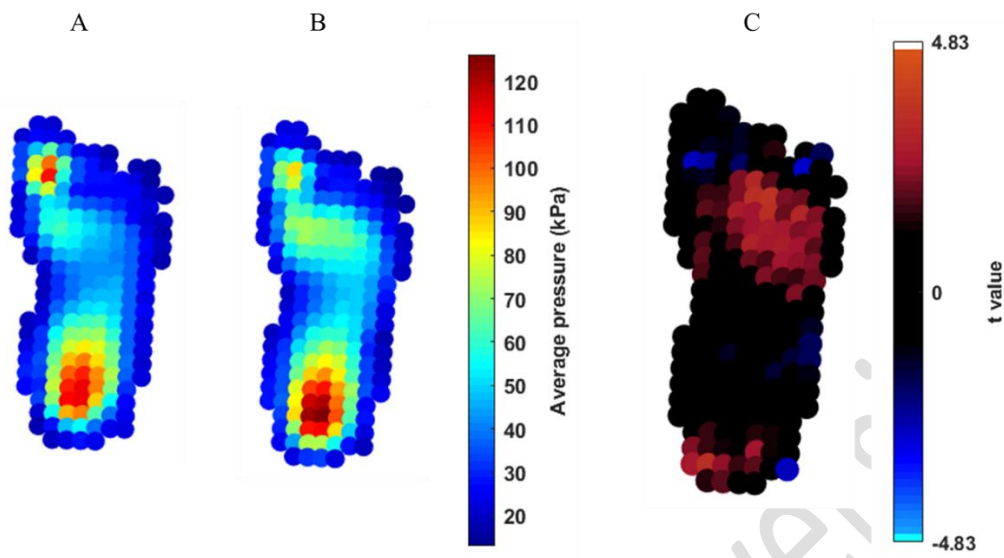
374

375

376

Fig. 4. Nonparametric pSPM paired t test on left feet for comparison between new and confident walking steps. From left to right: average pressure distribution of new walking (A), average pressure distribution of confident walking (B), and raw t value of statistical analysis (C), where the extremes of the colourbar reflects t-values needed to reach statistical significance, with alpha set at 0.05. The colourbar for A and B presented different min and max kPa values that were adjusted by the overall max and min values to allow for comparison. Cool and warm colours identify where confident walking steps had lower and higher peak pressure than new walking steps, respectively (C).

377



378

379 Fig. 5. Nonparametric pSPM paired t test on the right feet for comparison between new and confident walking
380 steps. From left to right: average pressure distribution of new walking (A), average pressure distribution of
381 confident walking (B), and raw t value of statistical analysis (C), where the extremes of the colourbar reflects t-
382 values needed to reach statistical significance, with alpha set at 0.05. The colourbar for A and B presented
383 different min and max kPa values that were adjusted by the overall max and min values to allow for
384 comparison. Cool and warm colours identify where confident walking steps had lower and higher peak
385 pressure than new walking steps, respectively (C).

386

387